Sin, J. L., Fernandes, R., & Mercola, D. (1978) *Biochem. Biophys. Res. Commun. 82*, 1132.
Techima, Y., & Kakiuchi, S. (1974) *Biochem. Biophys. Res. Commun. 56*, 489.
Vanaman, T. C., Sharief, F., & Watterson, P. M. (1977) in *Calcium Binding Proteins and Calcium Function* (Wasserman, R. M., et al., Eds.) p 107, Elsevier, New York.
Walsh, M. (1978) Ph.D. Thesis, University of Manitoba.

Analysis of Cooperativity Observed in pH Titrations of Proton Nuclear Magnetic Resonances of Histidine Residues of Rabbit Cardiac Tropomyosin†

Brian F. P. Edwards‡ and Brian D. Sykes*

ABSTRACT: We have investigated in detail the cooperativity which we had previously observed in the pH titration profiles of the histidine residues of rabbit tropomyosin [Edwards, B. F. P., & Sykes, B. D. (1978) *Biochemistry 17*, 684]. Nonpolymerizing tropomyosin was prepared by carboxypeptidase digestion, and the titration profiles of its histidine residues were compared with those of undigested tropomyosin which was fully polymerized (in 0.1 M KCl) throughout the titration. We have concluded that both histidine-153 and histidine-273 have significant cooperativity in their pH titrations only in polymerized tropomyosin, that the cooperativity arises from an intrinsic pH-dependent conformational transition which links the two residues together and not from the known pH dependence of the polymerization, and that the best model for the cooperativity is a biallosteric adaption of the Monod–Wyman–Changeux formalism involving two classes of binding sites for the same ligand (protons). Three other models which postulated either a Hill transition, an interaction with a neighboring residue that also titrates, or a pH-dependent polymerization were also considered.

Tropomyosin molecules are found in the thin filaments of muscle sarcomeres where they function in the regulation of muscle contraction by calcium ions. The rodlike tropomyosin molecules (~420 by 20 Å; Caspar et al., 1969) form a continuous ribbon on both sides of the double helix of globular actin molecules by an end-to-end overlap of ~20 Å. Each tropomyosin rod covers seven actin molecules and has one troponin molecule bound to it (Hanson & Lowy, 1963; Ebashi et al., 1969). In resting muscle the tropomyosin molecules block the interaction between myosin and actin that generates tension. When calcium ions are temporarily released from the sarcoplasmic reticulum in response to a nerve impulse, troponin becomes saturated with calcium ions and undergoes a conformational change that moves the tropomyosin molecules to a nonblocking position. Harrington (1979) has recently reviewed the extensive literature on the mechanisms of muscle contraction and its regulation.

Tropomyosin is a coiled coil of two α-helical polypeptide chains, based upon theoretical considerations (Crick, 1953), measurements of optical rotary dispersion (Cohen & Szent-Gyorgyi, 1957), electron micrographs (Caspar et al., 1969), and the amino acid sequence (Stone & Smillie, 1978). The X-ray crystallographic structure at 20-Å resolution (Phillips et al., 1979) has confirmed the earlier work.

We have used ^{1}H nuclear magnetic resonance to investigate the relationship between the physical properties of purified tropomyosin molecules and their function on the thin filaments (Edwards et al., 1977; Edwards & Sykes, 1978, 1980). In our study of the resonances from the histidine residues of tropomyosin (Edwards & Sykes, 1978), we observed two anomalies which required further examination: (1) the resonance from the C-2 proton of histidine-153 broadened into a square multiplet of resonances under certain conditions, and (2) the pH titration profiles of the most up- and downfield resonances of this multiplet were cooperative. In that paper we suggested that the multiple resonances derived from interconverting conformations of differing pK_a. However, we postponed an analysis of the cooperativity because we did not know if the different resonances of the multiplet came from individual species.

We have since determined that the different conformational forms are associated with the thermal unfolding of the coiled coil (Edwards & Sykes, 1980). The C-2 resonances from histidine-153 and histidine-276 of α,α'-tropomyosin are single peaks at 34 °C and below so long as the protein is fully reduced. Formation of a cross-link between cysteine-190 and cysteine-190′ destabilizes the middle region of tropomyosin (Lehrer, 1978) and lowers the temperature at which the multiple histidine resonances appear. We have analyzed the pH titration profiles of the histidine C-2 resonances in the ^{1}H NMR spectra of this "low-temperature" conformation and found them still to be cooperative. In this paper we present a physical explanation for the cooperativity, and we discuss four models that could explain the data.

Experimental Procedures

We have recently presented our biochemical and NMR procedures in detail (Edwards & Sykes, 1980). All the experiments discussed in this paper used rabbit cardiac tropomyosin which has two identical α chains (Mak et al., 1979). The nonpolymerizing tropomyosin (αTM-NP) was prepared

† From the Medical Research Council Group on Protein Structure and Function and the Department of Biochemistry, University of Alberta, Edmonton, Alberta, Canada T6G 2H7. *Received December 10, 1980.* This work was supported by the Medical Research Council of Canada and the I. W. Killam Foundation (postdoctoral fellowship to B.F.P.E.).
‡ Present address: Biochemistry Department, Wayne State University, Detroit, MI 48201.

0006-2960/81/0420-4193$01.25/0

by digestion with carboxypeptidase A according to the methods of Tawada et al. (1975) as effected by Johnson & Smillie (1977).

The buffer for all the NMR samples was 40 mM K_2HPO_4, 1 mM EDTA,[1] 10 mM DTE, and either 0.1 or 1.0 M KCl. The pH measurements of the NMR samples were made at room temperature (24 °C); they were not corrected for being in D_2O. The NMR measurements were peformed at 28 °C.

We performed the pH titrations in two ways. In method 1 we titrated a single NMR sample (~0.4 mL) with small aliquots of 2 M DCl or NaOD. The pH at each point was read after spectrum acquisition with an Ingold microelectrode (Model 6030-04) attached to a Radiometer pH meter (Model 62). The meter was standardized on pH 7.0 buffer, and reference standards (Fisher; pH values 5.0, 6.0, 7.0, 8.0, and 9.0) were read immediately before the sample pH was measured. They were used to prepare a linear calibration curve from which the corrected value for the pH of the sample could be read. The sample was then adjusted to the next pH value and reinserted in the Bruker HX-270. Between measurements the pH electrode was cleaned with 0.1 M HCl and then kept in neutral buffer. In this method neither the samples nor the reference standards were stirred during the pH measurement.

We also performed several pH titrations in which the sample and the reference standards were stirred vigorously during the pH measurements (method 2). We began with a 5-mL sample of tropomyosin in the standard buffer and titrated it with 2 M DCl and NaOD. At each pH value we withdrew a 0.3-mL NMR sample. The larger volume allowed us to use a pH electrode (Radiometer GK2321C) which had a larger membrane area. The same reference standards as above were measured at the beginning, the middle, and the end of the titration. The dozen or so NMR samples were flushed with argon and stored in a refrigerater until they were needed.

Throughout each titration the DTE concentration was monitored with Ellman's reagent (Ellman, 1958) to ensure that the cysteines of tropomyosin were fully reduced. At the end of each titration the state of the cysteines was verified by carboxymethylation and amino acid analysis.

Models

We have successfully fit our data with the equations from three models of cooperative processes: a Hill model, an interacting neighbor model, and a biallosteric model. A fourth model, which assumed a pH-dependent, isodesmic polymerization for tropomyosin, was less successful and could be excluded by experiment. Its presentation has been relegated to the supplementary section of this paper (see paragraph at end of paper regarding supplementary material). We chose these models for our analysis because they cover a wide range of assumptions about the fundamental processes causing the cooperativity in our experiments. Each model gives an expression for the fractional protonation, Y, of a class of histidines which can be used to fit the observed chemical shifts, δ_{obsd}, of that class. Because the protonations are in the NMR fast-exchange limit (Markley, 1975), the observed chemical shift, δ_{obsd}, is

$$\delta_{obsd} = \delta_A + (\delta_{AH} - \delta_A)Y \quad (1)$$

where δ_A is the chemical shift of the resonance from unprotonated histidine, δ_{AH} is the corresponding chemical shift from protonated histidine, and Y is the fractional protonation of the histidine.

[1] Abbreviations used: EDTA, ethylenediaminetetraacetic acid; DTE, dithioerythritol; DSS, sodium 3-(trimethylsilyl)-1-propanesulfonic acid.

(I) Hill Model. Model I is a traditional measure of the cooperativity in protein–ligand interactions. It assumes the concerted binding of a nominal number (n) of ligands

$$A + nH \rightleftarrows AH_n \quad (2)$$

Only species A and AH_n are considered to exist in significant concentrations. The A species is a polymer with n or more actual binding sites. In the case of tropomyosin, whose monomer has two identical chains, no polymerization is necessary. The Hill expression for the fractional protonation (Markley, 1975) was derived in Edwards & Sykes (1978)

$$Y = \frac{[H]^n}{K_a^n + [H]^n} \quad (3)$$

The acid dissociation constant is K_a; the Hill coefficient is n. When $n = 1$, the equation is a standard Henderson–Hasselbach binding function.

(II) Interacting Neighbor Model. Shrager et al. (1972) developed expressions for analyzing cooperative titrations based upon the idea of a second residue which also titrates over the pH range of interest and which interacts with the residue that is being monitored. The two conformational states of the histidine residues are differentiated by whether or not the perturbing neighbor is protonated. The pK_a value of the histidine or its limiting chemical shifts, or both, will depend on which conformational state the histidine is in. The assumed equilibria are

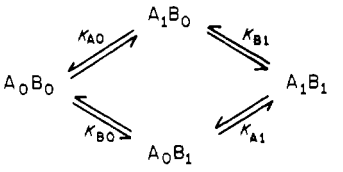

(4)

The general equation of the model, shown in eq 5, has five

$$\delta_{obsd} = \frac{a_1 + a_2[H] + a_3[H]^2}{1 + a_4[H] + a_5[H]^2} \quad (5)$$

coefficients, a_1–a_5, which incorporate the seven parameters of the unconstrained model. In our case, the histidine of interest is site A, and it has one set of values for the acid *association* constant, K_{A0}, and the limiting chemical shifts, δ_{A00} and δ_{A10}, when its perturbing neighbor is unprotonated and one set (K_{A1}, δ_{A01}, δ_{A11}) when the neighbor is protonated. The neighbor, itself, has one acid *association* constant, K_{B0}, when the histidine residue is unprotonated and a different one when the histidine is protonated, $K_{B1} = K_{A1}K_{B0}/K_{A0}$.

As discussed by Shrager et al. (1972), only two (δ_{A00} and δ_{A11}) of the seven parameters can be determined straightforwardly, and the other five parameters can only be calculated from the remaining coefficients by limiting the model in some way. There are two restricted cases of model II which are reasonable. Both assume that the increase in the chemical shift of the histidine residue upon protonation ($D = \delta_{AH} - \delta_A$) is independent of the perturbing neighbor ($\delta_{A10} = \delta_{A00} + D$, $\delta_{A01} = \delta_{A11} - D$).

Case 1 further assumes that the acid association constants are also independent of site B ($K_{A0} = K_{A1}$). With three unknowns, the problem is tractable.

Case 2 assumes that D is known, usually equal to the standard value of 0.95 ppm (Markley, 1975) or $\delta_{A11} - \delta_{A00}$, but it does not limit K_{A1}. All equations for model II are available as supplementary material.

(III) Biallosteric Model. Model III is developed from the concepts of Monod et al. (1965), extended to the case of two

Table I: Experimental Conditions of Titrations[a]

titration	sample	[KCl] (M)	method[b]
1	αTM-SH	0.1	1
2a	αTM-SH, GHG	0.1	1
2b	αTM-SH, GHG	0.1	2
3	αTM-SH	1.0	1
4	αTM-NP	0.1	1
5a	GHG	0.1	1
5b	GHG	0.1	2

[a] All samples had 40 mM K_2HPO_4, 1 mM EDTA, 10 mM DTE, 0.25 mM DSS, and 30 mg/mL tropomyosin. [b] See Experimental Procedures for an explanation of methods 1 and 2.

classes of sites whose fractional saturation by ligands can be measured separately. Edelstein & Gibson (1974) have published the specific equation for two binding sites in each class. Because we wished to vary the numbers of sites, we have derived the general equation; it follows conveniently from the derivation of the more usual case of a single class of sites (Monod et al., 1965). Both derivations are presented in detail in the supplementary material.

Our biallosteric model postulates a set of equilibria

$$(A_nB_m)_R \rightleftarrows (A_nB_m)_T \quad (6)$$

in which two classes of binding sites, A and B (e.g., His-153 and His-276), are converted by the same conformational change between their lower affinity form (T) and their higher affinity form (R) but are independent in their actual dissociation constants. In eq 6, the number of ligands (n) bound to the A sites can vary between 0 and the total number of A sites (N). Similarly, the number of ligands (m) bound to the B sites can vary between 0 and the total number of B sites (M). The assumption of independence means that in the equilibrium

$$(A_nB_m)_R \rightleftarrows (A_{n-1}B_m)_R + H \quad (7)$$

the dissociation constant K_R^A is independent of the number of ligands, m, bound at the B sites. The analogous assumption is made for K_T^A, K_R^B, and K_T^B.

The equations for the fractional saturation of the A and B sites (Y_A and Y_B) are

$$Y_A = \frac{a(1+a)^{N-1}(1+b)^M + c^A aL(1+c^A a)^{N-1}(1+c^B b)^M}{(1+a)^N(1+b)^M + L(1+c^A a)^N(1+c^B b)^M} \quad (8)$$

$$Y_B = \frac{b(1+b)^{M-1}(1+a)^N + c^B bL(1+c^B b)^{M-1}(1+c^A a)^N}{(1+a)^N(1+b)^M + L(1+c^A a)^N(1+c^B b)^M} \quad (9)$$

where N is the total number of A sites, M is the total number of B sites, a ($=[H]/K_R^A$ in our case) is the reduced ligand concentration for the A sites, b is the corresponding reduced ligand concentration for the B sites, L ($=[A_0B_0]_T/[A_0B_0]_R$) is the intrinsic allosteric equilibrium constant, c^A ($=K_R^A/K_T^A$) is the ratio of dissociation constants for the A sites, and c^B is the corresponding ratio for the B sites.

Results

From our earlier work (Edwards & Sykes, 1978, 1980) we suspected that the cooperativity in the histidine titration curves was related to the polymerization of tropomyosin because the Hill coefficients generally seemed to decrease with increased temperature or ionic strength. Table I outlines the experimental conditions of the five titrations which we have performed to examine this question. The concentration of DTE was above 5 mM in all the experiments, and the cysteines of the tropomyosin samples were fully reduced, within the error of the analysis, at the end of all the experiments. Oxidation of the DTE was significantly reduced by keeping argon above the samples and by storing them in a refrigerator until they were needed. We did not take these precautions in our earlier titrations of cardiac α,α′-tropomyosin (Edwards & Sykes, 1978; titrations 5–9); thus they had a mixture of reduced and oxidized tropomyosins, as shown by the multiple resonances for histidine-153 which were observed at 28 °C, even though the titrations began with 10 mM DTE in the samples.

Titrations 2 and 5 were done by titration method 2 (titrations 2b and 5b). After the NMR spectra had been taken, the pH values were measured again but in the NMR tube with the Ingold microelectrode without stirring (titrations 2a and 5a). The tropomyosin samples for titration 2 included 0.6 mM Gly-His-Gly (GHG) as a control.

We have analyzed the data from the five titrations by fitting them in a least-squares sense to the equations of one or more of the four models described above. Although in our discussion we argue that two of the models can be excluded from consideration for our particular case, we have analyzed the data of titration 1 with all four models because we were curious as to how well each model would fit the most cooperative data.

Model I. All five titrations were analyzed with the Hill equation; Tables II and III present the parameters from the least-squares fits using a program for derivative-free, nonlinear least-squares refinements written in the basic language (Hull, 1975). The estimated errors in the parameters of titration 4 were higher than the average because δ_{AH} could not be defined well due to isoelectric precipitation of the protein at the lower pH values. If δ_A and δ_{AH} were fixed at 7.68 and 8.62 ppm, respectively, the pK_a became 7.17 ± 0.03 and n became 1.08 ± 0.09.

In Figure 1, we have plotted the data for the most cooperative titration, namely, that of histidine-153 in titration 1, and have compared the titration curves predicted by the cooperative and noncooperative Hill equations. The parameters for the former came from Table II; the parameters for the latter came from a least-squares refinement in which n was fixed at 1.0 (δ_A = 7.63 ± 0.03 ppm, δ_{AH} = 8.68 ± 0.04 ppm,

Table II: Least-Squares Parameters for the Hill Model (I) for Tropomyosin Data

parameter	titration 1		titration 2a		titration 2b		titration 3		titration 4[a]	
	His-153	His-276	His-153	His-276	His-153	His-276	His-153	His-276	His-153	His-276
δ_A	7.69 ± 0.02	7.69 ± 0.02	7.72 ± 0.01	7.69 ± 0.01	7.71 ± 0.02	7.68 ± 0.01	7.68 ± 0.02	7.66 ± 0.02	7.66 ± 0.05	
δ_{AH}	8.58 ± 0.03	8.59 ± 0.02	8.60 ± 0.02	8.60 ± 0.01	8.61 ± 0.01	8.60 ± 0.01	8.67 ± 0.03	8.66 ± 0.03	8.64 ± 0.14	
pK_a	7.20 ± 0.03	7.35 ± 0.03	7.19 ± 0.02	7.38 ± 0.02	7.21 ± 0.03	7.42 ± 0.02	7.01 ± 0.04	7.13 ± 0.03	7.16 ± 0.13	
n	1.5 ± 0.2	1.3 ± 0.1	1.3 ± 0.1	1.14 ± 0.05	1.13 ± 0.07	1.05 ± 0.04	1.1 ± 0.1	1.01 ± 0.08	1.0 ± 0.3	
SE[b]	0.0395	0.0341	0.0155	0.0114	0.0153	0.0089	0.0249	0.0207	0.0474	

[a] The heterogeneity of the carboxy-terminal end of αTM-NP made the histidine-276 resonance too broad to assign. [b] The standard error is given by $[\Sigma(\delta_{obsd} - \delta_{calcd})^2/(N-P)]^{1/2}$ where N is the number of observations and P is the number of parameters in the equation. The sum is over all the observations.

Table III: Least-Squares Parameters for the Hill Model (I) for the GHG Data

parameter	titration 2a	titration 2b	titration 5a	titration 5b
δ_A	7.68 ± 0.01	7.67 ± 0.01	7.67 ± 0.01	7.67 ± 0.01
δ_{AH}	8.59 ± 0.01	8.63 ± 0.02	8.62 ± 0.01	8.62 ± 0.01
pK_a	6.91 ± 0.01	6.85 ± 0.03	6.79 ± 0.01	6.81 ± 0.01
n	0.98 ± 0.02	0.84 ± 0.04	0.92 ± 0.02	0.90 ± 0.01
SE	0.0036	0.0085	0.0059	0.0039

Table IV: Least-Squares Parameters for the Interacting Neighbor Model (II)

	titration 1		
parameter	His-153	His-276	titration 5a
a_1	7.71 ± 0.04	7.65 ± 0.02	7.67 ± 0.01
a_2[a]	16.0 ± 15	18.1 ± 2.7	19.6 ± 12
a_3[b]	54.5 ± 50	0.0	7.4 ± 7.3
a_4[a]	2.1 ± 2.0	2.09 ± 0.32	2.3 ± 1.5
a_5[b]	6.33 ± 5.8	0.0	0.86 ± 0.85
SE	0.0385	0.0389	0.0059

[a] Exponent is 10^7. [b] Exponent is 10^{14}.

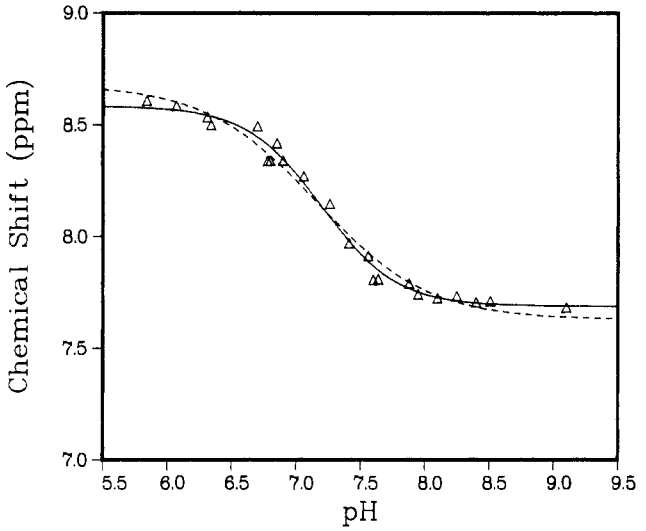

FIGURE 1: Titration curves predicted by the Hill equation for histidine-153 data of titration 1. The solid curve is calculated from the parameters of Table II (Hill coefficient of 1.5) while the broken curve is calculated from a least-squares refinement in which the Hill coefficient was fixed at 1.0, the noncooperative value.

pK_a = 7.16 ± 0.06, SE = 0.0511).

Model II. We used the BMDP3R computer program developed by the Health Sciences computing Facility of the University of California, Los Angeles, CA, to fit the data of titrations 1 and 5a to eq 5 in a least-squares sense (Table IV). However, the program worked smoothly only after we scaled the [H] values by 10^7 and set minima of 0.0 on all the parameters.

Model III. Because eq 8 and 9 are linked by common parameters, we analyzed the chemical shift data from titration 1 for histidine-153 and histidine-276 (sites A and B) simultaneously by using the Time Series Processor package of programs implemented at the University of Alberta. To achieve a smooth refinement, we were obliged to keep c^A and c^B positive by using their absolute values in eq 8 and 9 and to scale the [H] values by 10^7. Table V lists the refined parameters for titrations 1 and 4. Under the conditions of titration 1, tropomyosin is fully polymerized into dimers and higher oligomers (Tsao et al., 1951, Kay & Bailey, 1960). However, we decided to assume only dimers and set both N and M in eq 8 and 9 to 4. It was the most rigorous test of the model because cooperativity is more easily modeled as the number of sites is increased. Under the conditions of titration 4, tropomyosin is monomeric. We set N and M equal to 2 but assumed that the dissociation constants (K_R^A, K_R^B, K_T^A, and K_T^B) were unchanged from those of titration 1. This simultaneous rationalizaiton of the data from the polymerized and nonpolymerized tropomyosin by a common set of parameters is shown in Figure 2 for histidine-153. We could not assign a resonance to histidine-276 on the digested, nonpolymerizing tropomyosin.

Table V: Least-Squares Parameters for the Biallosteric Model (III)

parameter	titration 2	titration 4
K_R^A	(0.44 ± 0.06) × 10^{-7}	
c^A	0.20 ± 0.08	
K_R^B	(0.36 ± 0.04) × 10^{-7}	
c^B	0.49 ± 0.07	
L	20.2 ± 15	2.6 ± 0.7
SE	0.031	0.044

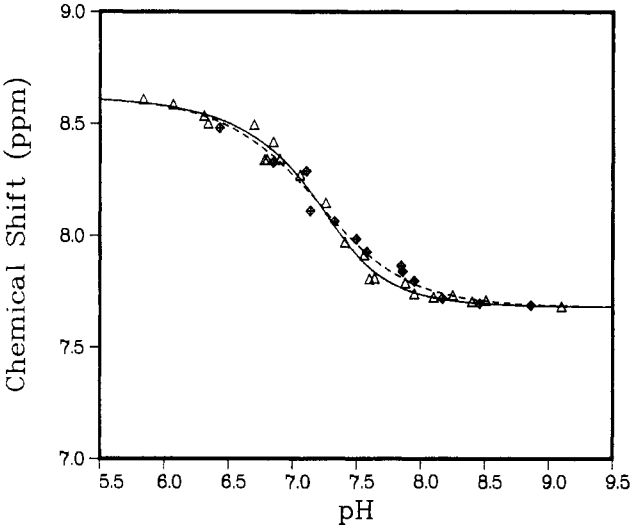

FIGURE 2: Histidine-153 data from titration 1 (△) and titration 4 (◇) showing their respective predictions as solid and broken curves, by the biallosteric model using the parameters of Table V.

Discussion

The numbers in Tables II and III show that titration method 1 (no stirring during pH measurements) gave higher cooperativities than method 2. We attribute most of this difference to systematic differences in the pH measurements, rather than in the chemical shift values, because the NMR spectra were recorded under identical conditions for all the titrations.

Morever, the Hill coefficients from titration 2b were underestimated since the Hill coefficient for its GHG resonance is lower than that of GHG in titration 5b. A "standard" titration profile is noncooperative with a Hill coefficient of 1.0. The negative cooperativity (Hill coefficient <1.0) of the GHG titrations at low ionic strengths is caused by the α-amino group whose pK_a is 8.15 in water at 0.15–0.19 M ionic strength (Rabenstein et al., 1977). A theoretical titration curve that was calculated from the microscopic acid dissociation constants of Rabenstein et al. (1977) had a Hill coefficient of 0.94 ± 0.01. Consequently, our experiments have assigned bonds of 1.1–1.5 for the Hill coefficients of the titration curves of the histidines of α,α'-tropomyosin at 28 °C and an ionic strength of 0.2 M.

The numbers in Table II also show that depolymerizing the protein by enzymatic digestion (titration 4) or by higher ionic

strength (titration 3) will reduce the cooperativity of the titration to essentially nil, even though method 1, by which they were done, favors cooperativity. We did not titrate more dilute solutions of tropomyosin at low ionic strength because the signal-to-noise ratio was too low. Moreover, other researchers have shown that tropomyosin is mostly polymerized in 0.1 M KCl, even at 1 mg/mL (Tsao et al., 1951; Kay & Bailey, 1960; Ooi et al., 1962).

Our NMR titration data are essentially individual fractional saturation curves for the binding of protons to two specific sites, namely, histidine-153 and histidine-276, on tropomyosin. The cooperative binding curves imply that the histidine residues of tropomyosin have at least two conformational states in which they each have either different affinities for protons or different limiting chemical shifts, δ_A and δ_{AH}, or both conditions simultaneously. Over the pH range of the titrations, the histidine residues must move from being predominantly in the "basic" conformation to being predominantly in the "acidic", or the reverse, depending upon the direction of the titration.

We have evalulated three other models, besides the Hill equation, for their ability to predict and rationalize our cooperative pH titration data. We have used titration 1 as the test case because its data exhibit the greatest range of cooperativity and thus demand the most of any model.

Five constraints, implied by the parameters of Tables II and III and by some additional physicochemical information, have guided our application of the models. First, we have accepted that *both* histidine-153 and histidine-276 show cooperative titrations, although the latter is only weakly so. Second, because depolymerization reduces the cooperativity for both histidine-153 and histidine-276 in titrations 3 and 4, we consider it likely that the two histidines, separated by over 180 Å, derive their cooperativity from a common conformational transition. Third, the differences between the limiting chemical shifts of the cooperative titrations and those of standard histidines such as GHG are small and within experimental error. For instance, although δ_A and δ_{AH} for histidine-153 in titration 1 were 7.69 and 8.58, respectively, the minimum and maximum chemical shifts that were actually measured were 7.68 and 8.61 ppm. Since most of the uncertainty in our data came from the pH measurements, the observed chemical shifts are probably better estimates of δ_A and δ_{AH} than the values derived from the least-squares fits. Fourth, the cooperativity is positive. Fifth, as mentioned already, tropomyosin is completely polymerized under the conditions of ionic strength and protein concentration used for titration 1.

The last point excluded the fourth model (supplementary material) which was based upon a pH-dependent polymerization of tropomyosin. For production of sufficient cooperativity, it demanded that tropomyosin go from completely monomer to completely polymer over the pH range of interest. Although Ooi et al. (1962) found that very dilute solutions of tropomyosin were less polymerized at pH 6 than at pH 8, we could not establish sedimentation equilibrium at pH 6.0 with a 10 mg/mL solution of tropomyosin in our usual D_2O buffer. The rotor speed on the Beckman Model E ultracentrifuge was 1600 rpm. By our experiment and those in the literature, the tropomyosin molecules are fully polymerized under the conditions of titration 1.

Taken together, these constraints favor models I and III. We have used the Hill equation of model I as a mathematically convenient and traditional way to measure the deviation from a standard titration. However, not only does it give an excellent numerical fit to all our data but also it can rationalize the effects of depolymerization by assuming that the monomer, which has two possible binding sites (histidine residues) of each type, has a slight cooperativity that is greatly amplified in the polymer which could have 12 or more sites of each type (Kay & Bailey, 1960).

Model II gave stable refinements by least squares for titration 1 (Table IV), although coefficients a_2 to a_5 had large estimated errors in all refinements because they were strongly correlated with one another. For titration 1, the refinement yielded reasonable values for δ_{A00} and δ_{A11} (7.71 and 8.61 ppm, respectively), but under the assumptions of case 1 of model II it gave an imaginary value for K_{A0}, and under the usual assumptions of case 2 of model II ($D = 0.95$ ppm or $D = \delta_{A11} - \delta_{A00} = 0.90$ ppm) it gave a negative value for K_{A0}. If K_{A0} was set to a lower bound of 10^6 M^{-1}, then case 2 gave the ostensibly reasonable values of 3.2×10^7 M^{-1} for K_{A1}, 2.0×10^7 M^{-1} for K_{B0}, and 1.07 ppm for D. However, these values are still physically unreasonable because K_{A0} is less than K_{A1}; both carboxyl and amino groups (including histidines), which are the only available candidates for site B in model II, would *decrease* the association constant of a nearby histidine as they became protonated ($K_{A0} > K_{A1}$) and cause negative cooperativity.

Model II is also aesthetically unappealing for titration 1. The concept of a localized cause is strained by the observation that both histidines are cooperative and that both are affected by carboxypeptidase digestion of the C-terminal end, although only histidine-276 is near it. A possible alternative is to assume that some group near the C-terminal end of tropomyosin controls a conformational change that extends over the entire molecule. But such an assumption is antithetical to the spirit of this "local" model; it fits more naturally into the concepts of model III.

For comparison, we also applied model II to one of the GHG titrations (5a) for which it should be the proper model. Case 2, with $D = \delta_{A11} - \delta_{A00}$, gave a set of values ($\delta_{A00} = 7.67$ ppm; $\delta_{A11} = 8.60$ ppm; $K_{A0} = 0.81 \times 10^7$ M^{-1}; $K_{A1} = 0.56 \times 10^7$ M^{-1}; $K_{B10} = 1.52 \times 10^7$ M^{-1}) in which the association constants agreed well with the results of Rabenstein et al. (1977) in their trends ($K_{B0} > K_{A0} > K_{A1}$) but only approximately in their values (K_{A0} = antilog $pK_{123} = 1.4 \times 10^7$ M^{-1}; K_{A1} = antilog $pK_{13} = 0.46 \times 10^7$ M^{-1}; K_{B0} = antilog $pK_{132} = 12.3 \times 10^7$ M^{-1}). Such disagreement is not unexpected given the very high estimated errors in our coefficients, a_2–a_5. Strong correlations among the parameters produced the high estimated errors and made eq 5 difficult to refine.

We have found that the biallosteric model (model III) agrees best with our data. The parameters are reasonable and the effects of depolymerization by carboxypeptidase digestion or by increased ionic strength can be comfortably incorporated. We need only assume that the low (T) and high (R) affinity conformations are accessible to both monomer and polymer but that polymerization favors (increases L) the T conformation in which the histidines have a lower affinity for protons.

The nature of these conformations is uncertain. We have previously shown that both histidines have coexisting conformations in which they exhibit different pK_a values during the thermal unfolding of tropomyosin (Edwards & Sykes, 1980). However, those conformations were in the NMR slow-exchange limit whereas the transitions that cause the cooperativity must be in the fast-exchange limit, since we see only one resonance for each type of histidine. The two sets of transitions could be connected since histidine-153, which exhibits the greater cooperativity here, is near a region of instability in the coiled coil of tropomyosin (Lehrer, 1978) which makes it the first of the two histidines to show the

multiple conformations during thermal unfolding.

Acknowledgments

This work has benefited greatly from the interest and advice of Dr. C. M. Kay and of Dr. L. B. Smillie and members of his research group, especially Dr. W. Lewis and Dr. A. Mak. We are indebted to Dr. Marius Brouer for bringing the paper of Edelstein and Gibson (Edelstein & Gibson, 1974) to our attention. We are fortunate to have had the excellent technical assistance of M. Natriss for the amino acid analyses and M. Aarbo for the analytical centrifugation runs.

Supplementary Material Available

The derivation of eq 8 and 9 of the biallosteric model, the equations for model II, and the derivations, results, and discussion of model IV (17 pages). Ordering formation is given on any current masthead page.

References

Caspar, D. L. D., Cohen, C., & Longley, W. (1969) *J. Mol. Biol. 41*, 87.
Cohen, C., & Szent-Gyorgyi, A. G. (1957) *J. Am. Chem. Soc. 79*, 248.
Crick, F. H. C. (1953) *Acta Crystallogr. 6*, 689.
Ebashi, S., Endo, M., & Ohtsuki, I. (1969) *Q. Rev. Biophys. 2*, 351.
Edelstein, S. J., & Gibson, Q. H. (1975) *J. Biol. Chem. 250*, 961.
Edwards, B. F. P., & Sykes, B. D. (1978) *Biochemistry 17*, 684.
Edwards, B. F. P., & Sykes, B. D. (1980) *Biochemistry 19*, 2577.
Edwards, B. F. P., Lee, L., & Sykes, B. D. (1977) in *Cellular Function and Molecular Structure* (Agris, P. F., Ed.) Academic Press, New York.
Ellman, G. (1958) *Arch. Biochem. Biophys. 74*, 443.
Hanson, J., & Lowy, J. (1963) *J. Mol. Biol. 6*, 46.
Harrington, W. F. (1979) *Proteins (3rd Ed.) 4*, 246.
Hull, W. (1975) Ph.D. Thesis, Harvard Univeristy, Cambridge, MA.
Johnson, P., & Smillie, L. B. (1977) *Biochemistry 16*, 2264.
Kay, C. M., & Bailey, K. (1960) *Biochim. Biophys. Acta 40*, 149.
Lehrer, S. S. (1978) *J. Mol. Biol. 118*, 209.
Mak, A. S., Lewis, W. G., & Smillie, L. B. (1979) *FEBS Lett. 105*, 232.
Markley, J. L. (1975) *Acc. Chem. Res. 8*, 70.
Monod, J., Wyman, J., & Changeux, J.-P. (1965) *J. Mol. Biol. 12*, 88.
Ooi, T., Mihashi, K., & Kobayushi, H. (1962) *Arch. Biochem. Biophys. 98*, 1.
Phillips, G. N., Lattman, E. E., Cummins, P., Lee, K. Y., & Cohen, C. (1979) *Nature (London) 278*, 413.
Rabenstein, D. L., Greenberg, M. S., & Evans, C. A. (1977) *Biochemistry 16*, 977.
Shrager, R. I., Cohen, J. S., Heller, S. R., Sachs, D. H., & Shecter, A. (1972) *Biochemistry 11*, 541.
Stone, D., & Smillie, L. B. (1978) *J. Biol. Chem. 253*, 1137.
Tawada, Y., Ohara, H., Ooi, T., & Tawada, K. (1975) *J. Biochem. (Tokyo) 78*, 65.
Tsao, T.-C., Bailey, K., & Adair, G. S. (1951) *Biochem. J. 49*, 27.

Potassium Ion Is Required for the Generation of pH-Dependent Membrane Potential and ΔpH by the Marine Bacterium *Vibrio alginolyticus*†

Hajime Tokuda,* Tatsunosuke Nakamura, and Tsutomu Unemoto

ABSTRACT: The electrochemical potential gradient of protons in the marine bacterium *Vibrio alginolyticus* was measured as a function of external pH. In K^+-containing cells, the membrane potential ($\Delta\psi$) and ΔpH vary with external pH as reported in other bacteria. On the other hand, K^+-depleted cells show little pH dependence in the magnitude of $\Delta\psi$ from pH 6.0 to 8.5. The cytoplasmic pH in these cells varies depending on external pH, resulting in the generation of a small ΔpH at acidic pH. Addition of K^+ to K^+-depleted cells leads to partial dissipation of $\Delta\psi$ and concomitant generation of ΔpH. Strikingly, this effect of K^+ is dependent on external pH. Collapse of $\Delta\psi$ and generation of ΔpH by the addition of K^+ decrease with increasing external pH. Thus, the $\Delta\psi$ and ΔpH obtained after addition of K^+ are essentially the same as those determined in K^+-containing cells, and cytoplasmic pH becomes less dependent on external pH. The results suggest that the variation of $\Delta\psi$ and ΔpH with external pH is controlled by K^+ transport.

The gram-negative marine bacterium *Vibrio alginolyticus* requires Na^+ for growth, and 0.3–0.5 M NaCl is optimal. When cells are grown on medium containing 0.3 M NaCl, the internal K^+ concentration is about 0.4 M, which is about 30-fold higher than that of the medium. On the other hand, the internal concentration of Na^+ is only about 0.1 M. Apparently, energy is required to maintain the internal ion compositions against their concentration gradients. Recently, evidence demonstrating the involvement of the proton motive force in K^+ uptake (Rhoads & Epstein, 1977; Wagner et al., 1978; Bakker & Harold, 1980) and Na^+ extrusion (West & Mitchell, 1974; Lanyi et al., 1976; Tokuda & Kaback, 1977; Schuldiner & Fishkes, 1978; Bhattacharyya & Barnes, 1978; Brey et al., 1978; Niven & MacLeod, 1978; Krulwich et al., 1979) has been presented for various bacteria. Therefore, it was of interest to examine the role of the proton motive force in the maintenance of internal ionic environment and, conversely, the effect of ionic environment on the formation of the proton motive force in *V. alginolyticus*.

According to the chemiosmotic hypothesis of Mitchell (Mitchell, 1968; Harold, 1977; Rosen & Kashket, 1978),

† From the Departments of Membrane Biochemistry (H.T. and T.U.) and Enzymology (T.N.), Research Institute for Chemobiodynamics, Chiba University, 1-8-1 Inohana, Chiba, Japan. *Received November 25, 1980.*

0006-2960/81/0420-4198$01.25/0